AMERICAN ACADEMY OF OPHTHALMOLOGY®

Long-Term Shape, Curvature, and Depth Changes of the Lamina Cribrosa after Trabeculectomy

Aistė Kadziauskienė, MD,[1,2] *Ernesta Jašinskienė, MD,*[2] *Rimvydas Ašoklis, MD, PhD,*[1,2] *Eugenijus Lesinskas, MD, PhD,*[1,2] *Tomas Rekašius, PhD,*[3] *Jacqueline Chua, BOptom, PhD,*[4,5] *Ching-Yu Cheng, MD, PhD,*[4,5,6] *Jean Martial Mari, PhD,*[7] *Michaël J.A. Girard, MSc, PhD,*[4,8] *Leopold Schmetterer, PhD*[4,5,9,10,11]

Purpose: To evaluate changes in lamina cribrosa (LC) shape, curvature, and depth after trabeculectomy.

Design: Prospective, observational case series.

Participants: A total of 112 patients (118 eyes) with open- or closed-angle glaucoma undergoing trabeculectomy.

Methods: The optic nerve head was imaged using enhanced depth imaging spectral-domain OCT before trabeculectomy and at 6 follow-up visits throughout the first postoperative year. The anterior LC surface and Bruch's membrane opening were marked in the serial horizontal B scans for the analysis of LC parameters using Morphology 1.0 software. Postoperative morphologic LC changes were assessed.

Main Outcome Measures: The postoperative LC global shape index (GSI), nasal-temporal (N-T) and superior-inferior (S-I) curvatures, and mean and sectoral LC depth (LCD).

Results: The mean LC GSI increased only during the early postoperative period ($P = 0.02$), resulting in a change toward the saddle-rut shape. There was a flattening of the LC curvature in N-T ($P < 0.001$) and S-I ($P = 0.003$) meridians 12 months after trabeculectomy. A shallowing of the mean and sectoral LCD from baseline was significant throughout the entire follow-up period ($P < 0.001$) and progressed up to postoperative month 6. Twenty-eight patients showed a deepening of the LC from baseline in at least 1 visit. Eyes with shallower LCD compared with baseline responded to intraocular pressure (IOP) reduction with greater movement anteriorly than eyes with deeper LCD ($P = 0.002$). Greater IOP reduction ($P = 0.007$), less retinal nerve fiber layer thinning over the year ($P = 0.003$), and more superiorly-inferiorly curved baseline LC ($P = 0.001$) were associated with an increase in GSI. Younger age and IOP reduction were related to LC shallowing ($P < 0.001$, $P = 0.002$) and N-T flattening ($P < 0.001$).

Conclusions: In most eyes, trabeculectomy resulted in long-term flattening and shallowing of the LC. However, in some eyes, LC deepened from baseline. Change in LC global shape appeared to be temporal. Reduction in IOP plays an important role in the early phase of LC change; however, in the later phase, LC remodeling may play a crucial role in view of stable IOP. *Ophthalmology 2018;■:1–12 © 2018 by the American Academy of Ophthalmology*

Supplemental material available at www.aaojournal.org.

To date, an elevated intraocular pressure (IOP) is proved to be the principal manageable risk factor for the development and progression of glaucoma.[1-5] However, the exact mechanism of IOP contributing to the glaucomatous injury remains incompletely understood. The lamina cribrosa (LC) is implicated to be the principal site of this damage.[6-11] Intraocular pressure is thought to affect the structures of the optic nerve head (ONH) directly as the determinant of translaminar pressure gradient and indirectly via the induced forces of the sclera.[12-14] Therefore, the connective tissues of the ONH, including the LC, scleral canal, and peripapillary sclera, constantly bear the biomechanical load, which in certain circumstances results in stress and strain to the tissue.[15] The biomechanical paradigm of glaucoma postulates that elevated IOP causes LC compression, stretch, and shear, which lead to lamina deformations, strains on glial cells, and subsequent damage of the retinal ganglion cell axons.[16,17] Lamina cribrosa morphology is related to the onset and progression of glaucoma.[18-21] Thus, all morphologic parameters describing the biomechanics of LC in relation to IOP are of great importance to provide insights into the fundamental mechanisms of glaucoma pathogenesis and treatment.

For many years, the assessment of the IOP effect on LC was limited to ex vivo histomorphometrical studies,[11,22,23] experimental animal studies,[6,24,25] or theoretical

https://doi.org/10.1016/j.ophtha.2018.05.011
ISSN 0161-6420/18

models.[14,26-29] Advanced imaging technologies, such as enhanced depth imaging spectral-domain OCT, swept-source OCT, and adaptive optics, allowed in vivo visualization and quantitative evaluation of the deep ONH structures.[30-35] Since then, the structural and biomechanical characteristics of LC in glaucomatous eyes have been widely investigated in vivo. A posterior displacement, thinning, and local defects of the LC have been suggested to occur more often in glaucoma-affected eyes and to be related to the progression of the disease.[19,21,36-41] A number of studies have reported a decrease in LC depth (LCD) after IOP reduction in glaucomatous eyes.[42-46] So far, the main morphologic parameter in the analysis of the LC and IOP relationship has remained the depth of the LC, which has limitations because of its reference to the plane of Bruch's membrane opening (BMO) and subsequent reliance on the shifting thickness of the choroid.[47-50] In this context, the LC parameters describing the LC curvature and shape could play an important role as potential morphologic biomarkers independent of the reference plane. However, data about the IOP effect on the curvature and shape of the LC are limited. Only 1 study investigated the LC posterior bowing after glaucoma surgery and suggested that an LC curvature index might have value as a parameter relevant to ONH biomechanics.[51] The examined curvature index did not correspond to the actual LC curvature, and the authors referred to the change of the LC configuration as a change in curvature. At present, no research has addressed the global shape of the LC after IOP reduction, and this relationship remains to be determined.

The aim of our prospective observational study was to evaluate the long-term changes of the LC shape, curvature, and depth after trabeculectomy. The recently introduced morphologic measure, the global shape index (GSI), was chosen to characterize the geometric shape of the anterior LC surface as a whole independently from the BMO plane.[52] Actual LC curvatures were assessed along vertical and horizontal meridians. We also analyzed the possible determinants of the LC morphologic changes.

Methods

Subjects and Inclusion Criteria

A prospective observational study was performed from 2014 to 2017 at Vilnius University Hospital Santaros Klinikos. The approval of the Regional Research Ethics Committee was obtained, and all investigations followed the tenets of the Declaration of Helsinki. Consecutive patients who met eligibility criteria and signed a written informed consent were enrolled in the study. The inclusion criteria were as follows: (1) diagnosis of open- or closed-angle glaucoma; (2) trabeculectomy indicated because of progressing glaucoma or high risk of glaucoma progression; (3) best-corrected visual acuity of 0.1 or greater; and (4) refractive error from −6.0 diopters (D) to +6.0 D of sphere and ±3.0 D of cylinder. Exclusion criteria were prior intraocular surgery except phacoemulsification with intraocular lens implantation, other ophthalmological or neurologic diseases affecting the visual field (VF), and poor image quality because of opaque ocular media. Glaucoma was diagnosed by the presence of glaucomatous optic neuropathy (neuroretinal rim thinning, notching, or retinal nerve fiber layer [RNFL] defects) with or without associated glaucomatous VF defect. The glaucomatous VF defect was defined as Glaucoma Hemifield Test of standard automated perimetry outside normal limits or a cluster of at least 3 contiguous points on the pattern deviation plot with $P < 5\%$ and 1 with $P < 1\%$ probability of being normal, or a pattern standard deviation of <5%. The VF test was considered reliable if false-positive and false-negative errors were less than 33% and fixation losses were less than 20%. Initially, 130 glaucomatous eyes of 124 patients planned for trabeculectomy were enrolled; of these, 12 patients (12 eyes) were excluded because of LC visibility less than 70% (6 eyes), failure to attend more than 2 follow-up visits (3 eyes), failed trabeculectomy (2 eyes), and postoperative complications (1 eye). Finally, we analyzed the data of 112 patients (118 eyes). Ten of these patients missed 1 follow-up visit, and 1 patient missed 2 follow-up visits.

Examinations and Measurements

Each participant underwent the baseline examination including assessment of best-corrected visual acuity by Snellen chart, autorefractometry (Topcon KR-1 Auto Kerato-Refractometre, Topcon Medical Systems, Oakland, NJ), applanation tonometry (Goldmann tonometer, Haag-Streit AG, Koeniz, Switzerland), slit-lamp biomicroscopy, dilated stereoscopic examination of the fundus, partial optical coherence interferometry (IOL Master, Carl Zeiss Meditec, Dublin, CA), and spectral-domain OCT (Heidelberg Spectralis, Heidelberg Engineering, Dossenheim, Germany). One ophthalmologist examined the patients. Two VF tests of achromatic automated perimetry using 30-2 Swedish Interactive Threshold Algorithm Standard strategy (Humphrey visual field analyzer, Carl Zeiss Meditec, Dublin, CA) were performed within 1 month before the trabeculectomy and repeated 12 months postoperatively. The final VF data of 9 patients were missing. The glaucoma was staged on the basis of the standard automated perimetry: mild glaucoma (mean deviation [MD] >−6 decibels [dB], <25% of points are depressed <5%, and <10 points are depressed <1% on a pattern deviation plot, all points in the central 5° with sensitivity ≥15 dB); moderate glaucoma (MD >−12 dB, <50% of points are depressed <5% and <20 points are depressed <1% on the pattern deviation plot, only 1 hemifield have a point in the central 5° with sensitivity <15 dB, no points within 5° of fixation with sensitivity of 0 dB); severe glaucoma (MD ≤−12 dB, >50% of points are depressed <5% and >20 points are depressed <1% on the pattern deviation plot, points within the central 5° with sensitivity <15 dB in both hemifields, at least 1 point has sensitivity of 0 dB within 5° of fixation).

We evaluated the morphologic parameters of the LC and IOP within 10 days preoperatively and postoperatively and at 1, 3, 6, 9, and 12 months postoperatively. The Goldman applanation tonometry was performed immediately after the spectral-domain OCT. The mean of 2 IOP measurements spaced 1 minute apart was calculated. If 2 measurements differed by more than 2 mmHg, we took a third reading and averaged the 2 closest values.

All patients underwent a limbal-based trabeculectomy, with or without adjunctive 5-fluorouracile, following the same surgical protocol by 1 of 4 surgeons. Subsequently, needling with 5-fluorouracile was performed if failure of the filtrating bleb occurred. Only patients with reduced postsurgical IOP continued the study. The composition of the study sample regarding the diagnosis reflected the statistical data of the patients undergoing trabeculectomies at Vilnius University Hospital Santaros Klinikos during the recruitment phase.

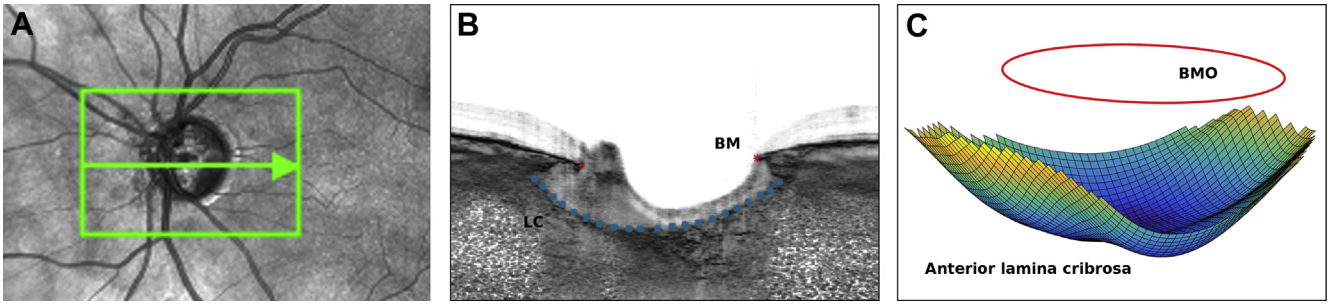

Figure 1. Imaging, delineation, and reconstruction of the lamina cribrosa (LC). We scanned the optic nerve head (ONH) by serial horizontal B scans spaced at approximately 63-μm intervals using enhanced depth imaging OCT. **A,** Infrared image of the ONH demonstrates the place of the horizontal section where the B scan was located. **B,** Cross-sectional view of the ONH after adaptive compensation (Reflectivity software, Ophthalmic Engineering & Innovation Laboratory, National University of Singapore, Singapore) and delineation of the anterior LC and end points of Bruch's membrane (BM) using Morphology 1.0 software (Ophthalmic Engineering & Innovation Laboratory, National University of Singapore, Singapore). **C,** Three-dimensional view of the reconstructed LC and plane of the Bruch's membrane opening (BMO).

Enhanced Depth Imaging OCT

One experienced ophthalmologist performed enhanced depth imaging spectral-domain OCT to visualize the LC.[30,33] The ONH was scanned with the Spectralis OCT system by centering a 15°×10° rectangle scan on the ONH. Each OCT volume consisted of 49 serial horizontal B scans (4.5-mm long lines, 40 images averaged) spaced at approximately 63-μm intervals. At least 2 OCT scans were taken, and the one with the best quality was chosen. Images with a quality score of 15 or less were excluded. The baseline OCT scan was set as a reference, and all subsequent scans done were adherent to it. Potential magnification error was avoided by entering the corneal curvature and refraction of the eye before the OCT scanning. The RNFL thickness was measured automatically from the circumferential OCT scan of 3.4 mm diameter centered at the ONH (single circle B scan of 12°, 100 images averaged).

Image Delineation, 3-Dimensional Reconstruction, and Morphologic Measurements of Lamina Cribrosa

We enhanced raw OCT images using adaptive compensation (Reflectivity software, version 3.4, Ophthalmic Engineering & Innovation Laboratory, National University of Singapore, Singapore). Such postprocessing has been shown to remove shadows, enhance tissue contrast, and improve the visibility of the LC.[53-55] Afterward, 2 ophthalmologists delineated and reconstructed the ONH volumes using semiautomated software Morphology 1.0 (version 1.0, Ophthalmic Engineering & Innovation Laboratory, National University of Singapore, Singapore). The anterior border of the LC was defined and manually marked on each B-scan as the upper margin of hyperreflective tissue below the ONH tissues extending laterally up to the LC insertions to the sclera (Fig 1). The regions with an undistinguishable LC border were not delineated. The Morphology 1.0 software determined the border of the LC area as the contour of all delineated points. On average, there were 259 (median, 258; range, 148–433) marked points per ONH scan included in the analysis. We also defined and delineated the BMO as the end points of hyperreflective Bruch's membrane layer on either side of the ONH in each B-scan. Subsequently, the Morphology 1.0 software 3-dimensionally reconstructed the LC anterior surface and BMO plane, and automatically calculated the morphologic parameters according to the earlier established protocols as follows.[52,56] The average LC visibility (LC coverage of BMO area evaluated by the software and expressed in %) of 130 enrolled eyes was 89.8% (median, 94.2; range, 29.8–97.8). Finally, 118 ONH scans with LC visibility of greater than 70% (mean, 92.4; median, 95.1; range, 71.3–97.8) were analyzed.

Lamina Cribrosa Depth. The software measured the LCD as the distance between the BMO plane and the anterior surface of the LC, which was reconstructed from the delineated LC points.[56] The mean LCD was calculated as the mean depth of all points on the LC surface. The lamina was automatically divided with respect to the center of BMO ellipse into 6 sectors, comprising four 45° sectors (superotemporal, superonasal, inferotemporal, and inferonasal) and two 90° sectors (temporal and nasal), and sectoral LCD was assessed.

Lamina Cribrosa Curvature. The LC curvature was measured in 2 principal meridians: S-I and N-T. The anterior LC surface was first intersected with 180 radial cross-sections that passed through the center of the BMO ellipse perpendicularly to it. An LC curve for each cross-section was generated.[52] Then, a circular arc was fitted to the LC curves along S-I and N-T directions. This approach enables estimation of LC curvatures along different radial orientations in a global sense without compromising robustness.[52] We expressed the values in mm^{1}, with negative values describing posteriorly curved LC and positive values indicating anteriorly curved LC.

Lamina Cribrosa Global Shape Index. The LC GSI assessment was based on global curvature measurements along radial LC directions and defined as

$$GSI = \frac{2}{\pi}\tan^{-1}\frac{\kappa_1+\kappa_2}{\kappa_1-\kappa_2}\ (\kappa_1 \geq \kappa_2)$$

where κ_1 and κ_2 are maximum and minimum principal arc curvatures of LC, respectively.[52] The value of the LC GSI varies

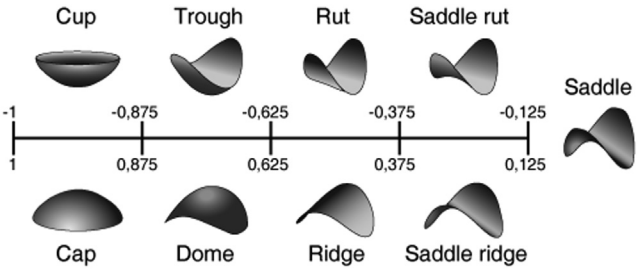

Figure 2. Global shape index (GSI) scale of LC representing 9 intervals with corresponding shapes. Modified from Thakku et al.[52]

between −1 and 1 and corresponds to a transition from spherical cup (posteriorly curved LC; GSI = −1) through a symmetric saddle-shaped LC (GSI = 0) to spherical cap (anteriorly curved LC; GSI = 1). Figure 2 demonstrates the scale of LC GSI with corresponding LC shapes. This index has been validated as a LC global shape parameter by Thakku et al.[52]

The reproducibility of the LC measurements was determined on the basis of the LC GSI and LCD evaluation in 20 ONH scans and showed good intergrader (intraclass correlation coefficient [ICC], 0.948; 95% confidence interval [CI], 0.875−0.979; ICC, 0.991; 95% CI, 0.977−0.996, respectively) and intragrader (ICC, 0.986; 95% CI, 0.966−0.994; ICC, 0.999; 95% CI, 0.998−1.0, respectively) agreements.

Statistical Analysis

We analyzed the data using R statistical software. Continuous variables were described by mean and standard deviation. We used the Friedman rank-sum test and the Nemenyi post hoc test to compare the preoperative and postoperative measurements of IOP, LC shape, curvature, and depth. The significance test for the Pearson correlation coefficient was used to evaluate the correlation between the changes of morphologic LC parameters at each time point. We performed a linear mixed model analysis for longitudinal data to evaluate the associations between the changes of LC GSI, LC curvatures, and LCD with possible explanatory variables. In addition to age and sex, variables with $P < 0.1$ from the univariate models were included in the multivariate model. The multivariate models of GSI, LCD, and N-T curvature were adjusted for baseline RNFL thickness. For the subgroup analysis, we used generalized estimating equation models to evaluate the relationship between LCD changes and IOP reduction. A P value of < 0.05 was considered statistically significant.

Results

In total, we analyzed the data of 118 eyes (112 patients). The demographic and clinical baseline characteristics of the patients are presented in Table 1. The mean IOP was significantly reduced at all follow-up visits ($P < 0.001$) (Fig S3, available at www.aaojournal.org; Table 2). At the first follow-up, the IOP reduction was the greatest when compared with the later visits ($P < 0.001$) and stabilized after the first month ($P > 0.05$ in between the subsequent visits).

Changes in Morphologic Parameters of Lamina Cribrosa

The mean LC GSI changed from baseline only in the early postoperative period ($P = 0.02$) when the IOP reduction was the greatest (Fig 4, Table 3). Its positive shift represented the change toward the saddle-rut shape (less concave N-T meridian and closer to flat or anteriorly curved S-I axis). During the subsequent visits, the GSI changes from baseline were statistically insignificant; however, they also showed tendency to the saddle-rut shape.

There was a flattening of both N-T and S-I curvatures of the LC after the trabeculectomy ($P < 0.001$, $P = 0.006$, respectively) (Fig 4, Table 3). The N-T curvature flattened from baseline at all follow-up visits ($P < 0.001$). The flattening of S-I curvature was significant 1 week and 12 months postoperatively ($P = 0.001$, $P = 0.003$, respectively).

The mean and sectoral LCD decreased (shallowed) at all follow-up visits after the trabeculectomy ($P < 0.001$) (Fig 5, Table 3). After the mean LCD decreased until the sixth month, there were no significant changes in between the later visits. The trend of temporal sequence of LCD seemed to be consistent for all LCD parameters. Before the trabeculectomy, the superonasal sector of the LC was the deepest and the temporal LC was the shallowest when compared with the others ($P < 0.001$). During the early postoperative period, the LCD decreased more significantly in both superior sectors when compared with the inferior, nasal, and temporal ones ($P \leq 0.02$). After 1 year, the superonasal LCD showed the greatest decrease compared with other sectors ($P \leq 0.001$), except the superotemporal sector ($P = 0.21$); the LCD change was the least in the temporal sector when compared with others ($P \leq 0.006$).

The postoperative LCD decreased from baseline (shallowing of the LC) in the majority of the cases. However, 28 patients (35 visits) showed an increase in the LCD from baseline (deepening of the LC) in at least 1 visit during the follow-up period. Most of those with an increase in the LCD were observed during the first postoperative month and decreased significantly over time (P for trend < 0.001) (Table 4). In the group with a decreased postoperative LCD, the patients tended to be younger (66.4±8.1 years, $P = 0.002$) and have thinner baseline RNFL (51.9±12.6 μm, $P = 0.04$) compared with those eyes with an increased postoperative LCD (71.2±9.3 years, 59.7±16.7 μm, respectively). There were no significant differences in terms of gender, baseline IOP, axial length, VF MD, or baseline LC parameters between the eyes with decreased and increased postoperative LCD ($P > 0.05$). Reduction in IOP was related to greater LCD change in both groups. However, the effect was greater in eyes in which the LC became shallower ($\beta = 1.67$; 95% CI, 1.1−2.24; $P < 0.001$) than in eyes in which the LCD became deeper ($\beta = 0.84$; 95% CI, 0.31−1.36; $P = 0.002$) after the surgery. In other words, eyes with shallower LCD compared with baseline responded to IOP reduction with greater movement anteriorly than eyes with deeper LCD ($P = 0.002$).

The magnitude of changes in GSI correlated with flattening of the S-I curvature ($\rho = 0.517$, $\rho = 0.724$, $P < 0.001$) and shallowing of the mean LCD ($\rho = 0.363$, $\rho = 0.231$, $P < 0.05$) at the first and last visits, respectively. The correlation of change in GSI with the changes in the N-I curvature was significant only in the

Table 1. Patient Demographic and Clinical Characteristics

Baseline Characteristic	Value
Age, yrs	67.6±8.8
Male/female	54/58
BCVA, decimal scale	0.67±0.25
Refractive error, D	−0.4±2.0
Central corneal thickness, μm	520±33
Axial eye length, mm	23.63±0.92
VF MD, dB	−14.69±8.91
Global RNFL thickness, μm	53.7±4.6
Glaucoma type, % (eyes)	
Pseudoexfoliative	75.4 (89)
Primary open-angle	17.8 (21)
Primary angle-closure	6.8 (8)
Glaucoma stage, % (eyes)	
Preperimetric	3.4 (4)
Mild	13. 6 (16)
Moderate	16.1 (19)
Severe	66.9 (79)

BCVA = best-corrected visual acuity; D = diopters; dB = decibels; MD = mean deviation; RNFL = retinal nerve fiber layer; VF = visual field.
Values expressed as mean ± standard deviation, unless otherwise indicated.

Table 2. Intraocular Pressure before and after Glaucoma Surgery

	Baseline	After Trabeculectomy					
		3–10 Days	*1 Mo*	*3 Mos*	*6 Mos*	*9 Mos*	*12 Mos*
IOP, mmHg	27.6±6.7	9.2±3.9	12.8±4.2	12.6±3.4	12.6±3.2	13.2±3.4	13.5±3.7
IOP reduction,* mmHg	-	18.3±7.7	15.0±7.4	15.1±7.3	15.1±7.5	14.5±7.3	14.3±7.7
IOP reduction,* %	-	65.0±16.9	51.9±17.3	52.2±16.1	52.0±16.4	49.8±17.5	48.5±18.8

IOP = intraocular pressure.
Values are expressed as mean ± standard deviation.
*The IOP reduction from baseline, $P < 0.001$ at all follow-up visits. *P* values were obtained using pairwise comparisons of the Nemenyi multiple comparison test.

early postoperative period ($\rho = 0.351$, $P < 0.001$). There was a positive correlation between the flattening of both LC curvatures and the shallowing of LC during the entire follow-up period ($\rho = 0.647$, $\rho = 0.515$, $P < 0.001$, N-T and S-I curvatures after 12 months, respectively). The flattening of the LC at both principal meridians correlated with each other ($\rho = 0.258$, $P = 0.005$; $\rho = 0.275$, $P = 0.003$; $\rho = 0.232$, $P = 0.012$ within 10 days, 1 month, and 9 months after the surgery, respectively).

Factors Associated with Morphologic Lamina Cribrosa Changes

In univariate regression analysis, the postoperative LC GSI change toward a positive value (the direction of cap) was associated with the deeper, more superiorly-inferiorly curved preoperative LC and less RNFL thinning over a year; greater IOP reduction was a nearly significant factor (Table 5). In the multivariate model, preoperative LC curvature at the S-I meridian, IOP reduction, and postoperative RNFL thinning over 1 year remained associated with GSI after the adjustment for age, sex, and baseline RNFL thickness (variance inflation factors [VIFs] for all variables <2). This suggested that the postoperative RNFL thinning over 1 year was independent of baseline RNFL thickness.

Multivariate regression analysis showed an association between the flattening of the N-T curvature and younger age ($\beta = 3.23$ mm^{-1}/yr; 95% CI, 1.75–4.71; $P < 0.001$), lower baseline IOP ($\beta = 4.26$ mm^{-1}/mmHg; 95% CI, 0.049–8.03; $P = 0.029$), greater IOP reduction ($\beta = -5.92$ mm^{-1}/mmHg; 95% CI, −9.14 to −2.69; $P < 0.001$), and RNFL thinning over 1 year ($\beta = -4.22$ mm^{-1}/μm; 95% CI, −5.59 to −0.85; $P = 0.016$) (VIF <5). The postoperative flattening of S-I curvature was associated with more negative baseline GSI ($\beta = 489.19$ mm^{-1}/μm; 95% CI, 80.62–897.76; $P = 0.021$), deeper baseline LCD ($\beta = -2.25$ mm^{-1}/μm; 95% CI, −3.10 to −1.4; $P < 0.001$), and flatter baseline N-T curvature ($\beta = -0.77$ mm^{-1}/mm^{-1}, 95% CI, −1.36 to −0.17; $P = 0.013$) (VIF <2).

Younger age, greater IOP reduction, more anteriorly-posteriorly and nasally-temporally curved preoperative LC, and more negative baseline GSI were associated with a greater decrease of the mean LCD after trabeculectomy (VIF <5) (Table 6). The association of decrease of the mean LCD with lower baseline IOP was nearly significant ($\beta = -1.89$ μm/mmHg; 95% CI, −3.84 to −0.005; $P = 0.059$).

The greater decreases in the inferotemporal, superotemporal, and superonasal LCD were related to thinner corresponding regional baseline RNFL (inferotemporal: $\beta = -0.43$ μm/μm; 95% CI, −0.82 to 0.03; $P = 0.038$; superotemporal: $\beta = -0.67$ μm/μm; 95% CI, −1.32 to −0.01; $P = 0.049$; superonasal: $\beta = -0.84$ μm/μm; 95% CI, −1.65 to −0.03; $P = 0.045$). However, the relationship of inferonasal LCD was not significant, although a tendency was seen ($\beta = -0.56$ μm/μm; 95% CI, −1.17 to 0.04; $P = 0.07$).

Discussion

In this study, we evaluated the quantitative shape, curvature, and positional changes of the LC in glaucomatous eyes during 1 year after trabeculectomy. A long-term flattening of the LC curvature as well as shallowing of mean and sectoral LCD were observed. However, the overall LC shape, characterized by GSI, changed significantly only in the early postoperative period.

Thus far, the clinically measurable quantitative LC parameters related to the ONH biomechanics have been limited. Most of the studies addressing the LC morphology evaluated the position rather than the shape of the lamina. The LC was reported to be deeper in glaucomatous eyes compared with healthy eyes.[19,20,57-59] However, the predominant measurement of the LC morphology was LCD, defined with reference to the BMO plane and, therefore, carried potential bias. The reason is that BMO position is influenced by the choroidal thickness, which has been shown to vary with age, diurnal phase, and systemic health, as well as after IOP reduction.[47,48,50,60] Moreover, although the change in the LCD after IOP reduction reflected the positional reversal of the lamina, it did not necessarily describe the change in the LC curvature or shape because the migration of the LC insertion might be possible because of active ONH remodeling.[17,61] Examining other LC parameters characterizing its morphology independently from shifting anatomic landmarks remained the important scientific goal.

Recently, increased attention has been given to the curvature of the LC, because it describes the LC topography and is not affected by the choroidal thickness. Kim et al[62,63] reported that the LC posterior bowing, expressed as a LC curvature index, was increased in primary open-angle glaucoma (POAG) when compared with healthy control subjects and in hypertension glaucoma when compared with normal tension glaucoma. Later, the LC curvature index was shown to have a better discriminating capability index between POAG and healthy eyes than the LCD.[64] Only 1 study has addressed the effect of IOP reduction on the LC curvature.[51] Lee at al[51] evaluated eyes with POAG after trabeculectomy and found a decrease of the LC curvature

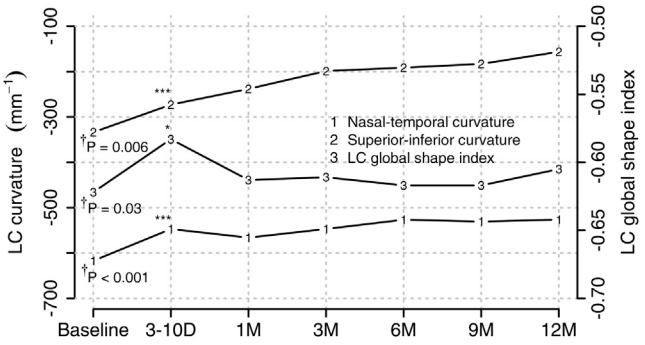

Figure 4. A line graph showing the time course of the lamina cribrosa global shape index (LC GSI), nasal-temporal (N-T), and superior-inferior (S-I) curvatures after trabeculectomy. There was a flattening of the N-T and S-I curvatures and an increase in GSI after surgery ($P < 0.001$, $P = 0.006$, $P = 0.03$, respectively). The N-T curvature flattened from baseline at all follow-up visits ($P < 0.001$). It was more curved at the first month when compared with curvature at 6, 9, and 12 months after surgery ($P = 0.01$, $P = 0.02$, $P = 0.002$, respectively) and at 3 months when compared with 12 months ($P = 0.03$). There were no changes in between the visits after 6 months. The S-I curvature was more curved at baseline when compared with 1 week and 12 months postoperatively ($P = 0.001$, $P = 0.003$, respectively); no changes were found in between other follow-ups. The GSI increased from baseline to the first follow-up ($P = 0.02$) and then decreased from the first follow-up to 3, 6, and 9 months ($P = 0.04$, $P = 0.049$, $P = 0.02$, respectively). †*P* values of the Friedman rank-sum test. **P* values for comparison with the previous follow-up obtained using the Nemenyi multiple comparison test. *$P \leq 0.05$. **$P \leq 0.01$. ***$P \leq 0.001$.

index in the horizontal ONH sections after surgical IOP reduction. The latter findings are in agreement with our study demonstrating the flattening of both principal LC curvatures; however, the results cannot be compared directly because in the previous study, the LC curvature index was defined as an inflection of the curve representing a section of the LC and did not correspond exactly to the actual LC curvature.[51] Furthermore, the measurements were limited to 7 horizontal cross-sections. In our study, a circular arc was fitted to each of the LC curves of radial cross-sections at principal meridians and allowed estimation of the LC curvature along radial orientations in a global sense.[52]

The LC GSI was introduced several years ago as a new morphologic parameter to characterize the geometric shape of the anterior lamina. The LC GSI does not depend on the BMO reference plane and gives a quantitative easily comparable value. In a healthy Indian population, the majority of the LC was reported to have the shape of a rut or saddle-rut and deeper LC insertions in the superior and inferior LC regions.[52] The GSI was shown to be smaller (more negative, toward the cup shape) in POAG eyes than in healthy or ocular hypertensive subjects.[56] In agreement, we also found the LC to be more curved in the N-T meridian compared with the S-I one and to be deeper in the superior and inferior LC sectors. However, the mean GSI values were smaller than previously described, indicating a shape shift toward the form of a cup. These differences are most likely due to the higher long-standing IOP and more advanced glaucoma of our subjects because glaucoma risk factors, such as vertical cup-to-disc ratio and minimum rim width, have been shown to be associated with more negative LC GSI.[52] In our study, the increase in LC GSI (shift toward the saddle-rut shape) was observed only in the early postoperative period at the time of the greatest IOP reduction. It is likely that later postoperative changes of the LC curvatures occurred concomitantly, because the GSI did not change significantly. Thus, this suggests that parameters such as LC curvature and LCD are clinically more relevant than GSI to describe the morphologic LC changes after trabeculectomy. However, the GSI parameter, but not LCD, has been reported to change during an IOP elevation in healthy and glaucomatous eyes.[56] Furthermore, eyes with POAG tended to have a more negative GSI during acute IOP increase than healthy eyes.

The positional responses of the LC to IOP changes have been evaluated in experimental and clinical studies reporting

Table 3. Shape, Curvature, and Depth Parameters of the Lamina Cribrosa during the Post-trabeculectomy Year

Parameter	Baseline	Postoperative						*P* Value
		3–10 Days	*1 Mo*	*3 Mos*	*6 Mos*	*9 Mos*	*12 Mos*	
N-T curvature, mm^{-1}	−617±191	−547±196	−566±186	−547±167	−527±162	−531±167	−526±163	<0.001
S-I curvature, mm^{-1}	−334±655	−273±699	−238±512	−199±455	−191±471	−183±417	−156±419	0.006
GSI	−0.622±0.18	−0.583±0.19	−0.613±0.19	−0.611±0.19	−0.617±0.18	−0.617±0.18	−0.605±0.19	0.03
Mean LCD, μm	449±129	412±112	410±108	400±104	385±100	384±100	383±101	<0.001
Sectoral LCD, μm								
Temporal	432±146	389±123	389±119	380±113	367±108	366±109	367±109	<0.001
Superotemporal	516±171	461±171	464±138	453±132	434±126	434±128	433±127	<0.001
Superonasal	546±173	491±146	494±140	481±134	462±129	461±131	458±128	<0.001
Nasal	499±153	455±131	454±124	442±119	425±113	422±114	422±115	<0.001
Inferonasal	493±153	455±137	445±127	436±125	420±119	417±119	419±122	<0.001
Inferotemporal	473±153	433±134	426±127	416±123	401±117	400±117	401±119	<0.001

GSI = global shape index; LCD = lamina cribrosa depth; N-T = nasal-temporal; S-I = superior-inferior.
Values are expressed as mean ± standard deviation.
P values were obtained with the Friedman rank-sum test.

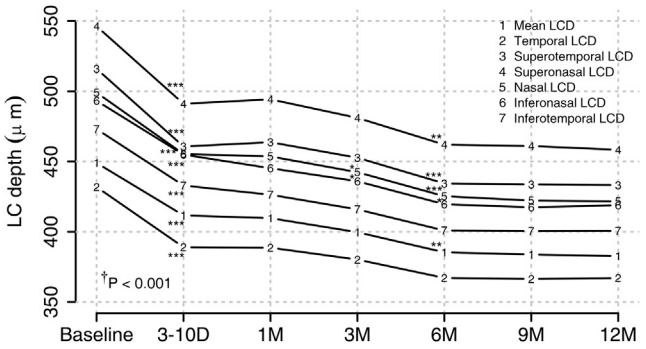

Figure 5. A line graph demonstrating the time course of mean and sectoral lamina cribrosa depth (LCD) after trabeculectomy. The mean and sectoral LCD decreased from baseline at all follow-ups ($P < 0.001$). The mean and sectoral LCD, except temporal and inferotemporal, were deeper at 1 week, 1 month, and 3 months when compared with 6, 9, and 12 months postoperatively ($P \leq 0.02$). There were no changes in between the visits after 6 months. †*P* values of the Friedman rank-sum test for all LCD parameters. **P* values for comparison with the previous follow-up visit obtained using the Nemenyi multiple comparison test. *$P \leq 0.05$. **$P \leq 0.01$. ***$P \leq 0.001$.

anterior-posterior displacements.[6,24,25,29,65] Most of them have observed a decrease in the mean LCD after IOP reduction.[44-46,66,67] However, several studies have previously reported that both posterior and anterior movements of the LC can occur after IOP lowering, which is in agreement with our data.[43,68,69] The different methodologies of measurements of the LCD and variable IOP reduction prevent direct comparison of the magnitude of LC change between different studies. Most of the research groups evaluated the LCD only in a selected number of the ONH scans where several parameters, usually representing the deepest, central, or paracentral LCD, were measured. In our study, improved image quality after adaptive compensation and custom-written software allowed us to cover approximately 90% of the lamina surface and to assess the mean depth including peripheral LC. That also enabled us to measure the sectoral LCD. We found the LCD to decrease more in the superior and inferior sectors when compared with the temporal segment. The smaller density of the supporting connective tissue and glial cells in the superior and inferior quadrants have been reported and could explain the difference in LC mobility.[70]

The mean postsurgical LCD in our study is comparable to the baseline data of Tun et al,[56] who evaluated LCD after IOP elevation in glaucomatous eyes using the same methodology. We found the mean LCD to decrease until postoperative month 6, and, thereafter, the LC position stabilized. These results are consistent with other authors reporting a similar tendency over a 6-month follow-up period.[66] Because IOP did not differ significantly between the visits after the first postoperative month, the subsequent changes of LCD and LC curvatures could be a result of connective tissue remodeling and collagen arrangement under new postoperative hydrostatic pressure circumstances.[17,71]

We have observed the inward and outward movements of the LC after trabeculectomy. In the majority of our patients, the LC became shallower. However, there was a small group of eyes that displayed a deepening of the LCD. Most of the cases with deeper LCD compared with baseline occurred within the first postoperative month and reduced in number over time. Such bidirectional biomechanical response of the LC to IOP change is a consequence of 2 major forces: the translaminar pressure gradient and IOP-induced circumferential forces of the peripapillary sclera affecting the LC.[12] Because of the decrease in translaminar and transscleral pressure gradients, we would assume the shallowing of the LC and inward movement of the peripapillary sclera after the IOP reduction. However, because the surrounding sclera and LC respond as a single unit, the altered scleral forces can subsequently influence the stresses and strains on the LC and, thus, induce its outward movement. The biomechanical behavior of LC and peripapillary sclera is not fully understood because of the complex interaction between the IOP, material properties, and geometry of LC and sclera.[29] This biomechanical variability of the LC is in agreement with model predictions by Sigal et al,[72] where the increase in LCD after IOP lowering could be explained by a reduction in scleral canal size leading to the posterior movement of the LC. Previous clinical studies have corroborated our findings that the LC moves anteriorly or posteriorly after a decrease in IOP.[43,44,68,69] Quigley et al[69] showed that the anterior LC position became shallower or deeper or stayed unchanged with IOP reduction. The displacement of LCD was greater at lower IOP but was not associated with the magnitude of IOP lowering. The eyes with no change in LCD tended to have greater VF loss than eyes with anterior LC reversal. Girard et al[68] evaluated the 3-dimensional ONH displacements and strain relief in vivo and found that the LC displaced posteriorly, anteriorly, or not at all; however, no factors related to different LC behavior were identified. In our study, we demonstrated that eyes with shallower LCD compared with baseline responded to IOP reduction with

Table 4. Proportions of Eyes According to the Change of Lamina Cribrosa Depth during Follow-up

Number of Eyes N (%)	3–10 Days	1 Mo	3 Mos	6 Mos	9 Mos	12 Mos
LCD decrease	107 (92.2)	103 (89.6)	112 (94.9)	110 (95.7)	116 (99.1)	114 (98.3)
LCD increase*	9 (7.8)	12 (10.4)	6 (5.1)	5 (4.3)	1 (0.9)	2 (1.7)

LCD = lamina cribrosa depth.
*The number of eyes with LCD increase reduced over time (*P* for trend < 0.001). *P* value was obtained using Cochran–Armitage test for trend.

Table 5. Regression Analysis of Factors Associated with the Postoperative Changes of the Lamina Cribrosa Global Shape Index

Variable	Change of LC GSI			
	Univariate		*Multivariate*	
	β (95% CI)	P	*β (95% CI)*	P
Age, yrs	−0.00007 (−0.002 to 0.002)	0.952	−0.0008 (−0.003 to 0.001)	0.491
Male sex	0.020 (−0.019 to 0.058)	0.324	0.028 (−0.006 to 0.062)	0.111
Axial length preoperative, mm	0.015 (−0.007 to 0.037)	0.175		
IOP preoperative, mmHg	−0.002 (−0.005 to 0.001)	0.186		
IOP reduction 1 yr postoperatively, mmHg	−0.002 (−0.005 to 0.0001)	0.061	−0.003 (−0.006 to −0.001)	0.007
CCT preoperative, μm	0.0001 (−0.0005 to 0.0007)	0.643		
VF MD preoperative, dB	0.001 (−0.001 to 0.003)	0.306		
VF MD decrease from baseline over 1 year, dB	0.003 (−0.007 to 0.012)	0.609		
RNFL thickness preoperative, μm	0.0007 (−0.0008 to 0.002)	0.368	−0.0006 (−0.002 to 0.001)	0.408
RNFL thinning from baseline over 1 year, μm	0.005 (0.0001–0.009)	0.047	0.007 (0.003–0.012)	0.003
BMO area preoperative, μm^2	0.026 (−0.023 to 0.076)	0.302		
LCD preoperative, μm	−0.0002 (−0.0003 to −0.00004)	0.013	0.00003 (−0.0002 to 0.0002)	0.719
N-T curvature preoperative, mm^{-1}	0.00006 (−0.00004 to 0.0002)	0.249		
S-I curvature preoperative, mm^{-1}	0.00007 (0.00004–0.0001)	<0.001	0.00006 (0.00003–0.0001)	0.001

BMO = Bruch's membrane opening; CCT = central corneal thickness; CI = confidence interval; dB = decibels; GSI = global shape index; IOP = intraocular pressure; LC = lamina cribrosa; LCD = lamina cribrosa depth; MD = mean deviation; N-T = nasal-temporal; RNFL = retinal nerve fiber layer; S-I = superior-inferior; VF = visual field.
In addition to age, sex, and baseline RNFL thickness, variables with $P < 0.1$ from the univariate model were included in the multivariate model.

greater movement anteriorly than eyes with deeper LCD. In agreement with earlier reported data for regional LC change after IOP lowering,[69] we found the preoperative RNFL to be thicker in eyes with posterior LC movement after surgery.

We also evaluated the relationships of the structural LC changes and their possible predictors. Younger age was a significant factor for the flattening and shallowing of the postoperative LC. The age-related differences in the extracellular matrix of the sclera and LC potentially leading to the changes in their material properties have been reported and could at least partly explain this association.[73] Studies in animal and human eyes have demonstrated that the sclera becomes stiffer with age and therefore is subject to higher stresses but lower strains at different levels of IOP;[74-77] still, there were contradictory results as well.[78] Albon et al[79,80] showed age-related changes in the collagenous and noncollagenous components of the LC and observed that the mechanical compliance of the human LC decreased with age. However, because the biomechanics of the LC and sclera are highly interdependent, it is difficult to isolate the effects on the biomechanical properties of the LC alone. Reduction in IOP was also associated with the decrease in

Table 6. Regression Analysis of Factors Associated with the Postoperative Changes of the Mean Lamina Cribrosa Depth

Variable	Change of Mean LCD (μm)			
	Univariate		*Multivariate*	
	β (95% CI)	P	*β (95% CI)*	P
Age, yrs	−2.76 (−3.88 to −1.65)	<0.001	−2.27 (−3.05 to −1.50)	<0.001
Male sex	−6.17 (−26.32 to 13.98)	0.550	−9.81 (−22.1 to 2.48)	0.121
Axial length preoperative, mm	3.40 (−8.01 to 14.80)	0.561		
IOP preoperative, mmHg	2.11 (0.67 to −3.55)	0.005	−1.89 (−3.84 to 0.05)	0.059
IOP reduction 1 yr postoperatively, mmHg	2.55 (1.33–3.77)	<0.001	2.78 (1.07–4.49)	0.002
CCT preoperative, μm	−0.15 (−0.45 to 0.16)	0.350		
VF MD preoperative, dB	−0.82 (−1.94 to 0.30)	0.156		
VF MD decrease from baseline over 1 year, dB	−1.62 (−6.38 to 3.14)	0.506		
RNFL thickness preoperative, μm	−0.81 (−1.54 to −0.09)	0.030	−0.0003 (−0.48 to 0.48)	0.999
RNFL thinning from baseline over 1 year, μm	1.20 (−1.21 to 3.61)	0.330		
BMO area preoperative, μm^2	−27.37 (−52.76 to −1.98)	0.037	6.10 (−11.23 to 23.43)	0.492
GSI preoperative, μm	−55.27 (−109.57 to −0.97)	0.049	52.29 (12.72 to 91.86)	0.011
N-T curvature preoperative, mm^{-1}	−0.15 (−0.20 to −0.11)	<0.001	−0.08 (−0.11 to −0.04)	<0.001
S-I curvature preoperative, mm^{-1}	−0.06 (−0.07 to −0.04)	<0.001	−0.05 (−0.06 to −0.03)	<0.001

BMO = Bruch's membrane opening; CCT = central corneal thickness; CI = confidence interval; dB = decibels; GSI = global shape index; IOP = intraocular pressure; LC = lamina cribrosa; LCD = lamina cribrosa depth; MD = mean deviation; N-T = nasal-temporal; RNFL = retinal nerve fiber layer; S-I = superior-inferior; VF = visual field.
In addition to age and sex, variables with $P < 0.1$ from the univariate model were included in the multivariate model.

LCD, curvature, and GSI after the surgery. Our findings are in agreement with the results of other authors reporting younger age and larger IOP reduction to be associated with greater changes in the LCD and curve after trabeculectomy.[44,45,51,66] However, the study of Quigley et al[69] showed that the LCD change was more related to the level of IOP than to the magnitude of IOP change.

We found RNFL thinning from baseline over 1 year to be associated with the changes of the LC shape and N-T curvature, but not the LCD. Lee and Kim[43] also did not report an association between the mean LCD reduction after trabeculectomy and the rate of progressive RNFL thinning. The explanations for the continuous RNFL thinning after trabeculectomy are not clear. The possibility that the progressive reduction in RNFL thickness is related to the loss of non nerve-fiber components of RNFL during the late stages of glaucoma cannot be denied. Although we do not have the reason for that, in our study the progressive RNFL thinning over 1 year, but not VF loss, appeared to be related to the morphologic changes of the LC after trabeculectomy. We could only hypothesize that RNFL thickness in eyes with very severe glaucoma may provide an estimate of the component of the RNFL thickness, which is not necessarily related to visual function.[81] The current study also found that thinner baseline RNFL was related to a greater decrease in LCD in the superior and inferotemporal regions. Our results are inconsistent with the previously reported finding;[69] however, given the complex biomechanical behavior of the ONH, it remains unclear why this is the case.

Study Strengths and Limitations

The semiautomated measurements of the global LC shape and actual geometric curvature, as well as the prospective design of the study with a long follow-up period, are obvious strengths of our study. However, we should note potential limitations. First, we performed only a horizontal scanning of the ONH, and the superior and inferior lamina were poorly visualized in a part of the peripheral scans. The mean LC visibility of the 130 enrolled eyes was 89.8%, which may be improved if one uses a radial scan approach. To minimize the limitation, only scans with LC visibility better than 70% (mean 92.4%) were analyzed. Second, the LC curvatures were measured in only 2 meridians, whereas the superior-temporal and inferior-temporal regions, which are prone to glaucomatous injury, were not evaluated. However, it has been reported that the sections containing the principal arc curvatures of LC are aligned to the vertical and horizontal directions.[52] Furthermore, a comparison of the GSI values computed from the entire reconstructed LC with the GSI values based on the N-T and S-I curvatures showed good agreement.[52] These results suggest that evaluation of the vertical and horizontal meridians alone would be sufficient to calculate GSI representing the LC global anterior shape. Third, the GSI was evaluated globally by fitting the arc curvature to the entire cross-section; thus, it did not reflect the local changes of LC shape. However, no widely accepted globally and locally sensitive parameter for LC geometry is available. Fourth, the mean and sectoral postoperative LCD measurements could be affected by the changing choroidal thickness, as was described previously.[50] Fifth, because of the small number of subjects with pre-perimetric disease, the subgroup analysis of preperimetric and perimetric glaucoma could not be performed. To see the differences of LC behavior after the trabeculectomy in eyes with and without associated VF loss, this question needs to be studied in a larger population. Sixth, the unequal sample sizes of pseudoexfoliative, POAG, and primary angle-closure glaucoma in the study population prevented us from comparing LC changes in different types of glaucoma. Because the majority of the patients receiving glaucoma surgery had pseudoexfoliative syndrome, the study sample mostly reflected the morphologic changes of LC in pseudoexfoliative glaucoma. This potentially could have influenced the results of the LC biomechanical response if considering a possible pseudoexfoliation-specific elastinopathy of the LC and findings that the lamina is thinner and less stiff in eyes with pseudoexfoliation syndrome.[82,83] Further studies are needed to overcome these limitations and investigate the long-term structural changes of the post-trabeculectomy LC morphology and its association with glaucomatous injury.

We conclude that in most eyes, trabeculectomy induced a continuous flattening and shallowing of the LC, which tended to stabilize after 6 months. However, in some eyes, the LCD deepened from baseline. Change in LC global shape appeared to be temporal. Reduction in IOP played an important role in the early phase of LC change; however, in the later phase, LC remodeling may have played a crucial role, in view of stable IOP.

References

1. Comparison of glaucomatous progression between untreated patients with normal-tension glaucoma and patients with therapeutically reduced intraocular pressures. Collaborative Normal-Tension Glaucoma Study Group. *Am J Ophthalmol*. 1998;126:487–497.
2. The Advanced Glaucoma Intervention Study (AGIS): 7. The relationship between control of intraocular pressure and visual field deterioration. The AGIS Investigators. *Am J Ophthalmol*. 2000;130:429–440.
3. Heijl A, Leske MC, Bengtsson B, et al. Reduction of intraocular pressure and glaucoma progression: results from the Early Manifest Glaucoma Trial. *Arch Ophthalmol*. 2002;120:1268–1279.
4. Kass MA, Heuer DK, Higginbotham EJ, et al. The Ocular Hypertension Treatment Study: a randomized trial determines that topical ocular hypotensive medication delays or prevents the onset of primary open-angle glaucoma. *Arch Ophthalmol*. 2002;120:701–713. discussion 829-830.
5. Musch DC, Gillespie BW, Niziol LM, et al. Intraocular pressure control and long-term visual field loss in the Collaborative Initial Glaucoma Treatment Study. *Ophthalmology*. 2011;118:1766–1773.

6. Bellezza AJ, Rintalan CJ, Thompson HW, et al. Deformation of the lamina cribrosa and anterior scleral canal wall in early experimental glaucoma. *Invest Ophthalmol Vis Sci*. 2003;44:623–637.
7. Burgoyne CF, Downs JC, Bellezza AJ, Hart RT. Three-dimensional reconstruction of normal and early glaucoma monkey optic nerve head connective tissues. *Invest Ophthalmol Vis Sci*. 2004;45:4388–4399.
8. Quigley HA, Addicks EM, Green WR, Maumenee AE. Optic nerve damage in human glaucoma. II. The site of injury and susceptibility to damage. *Arch Ophthalmol*. 1981;99:635–649.
9. Howell GR, Libby RT, Jakobs TC, et al. Axons of retinal ganglion cells are insulted in the optic nerve early in DBA/2J glaucoma. *J Cell Biol*. 2007;179:1523–1537.
10. Lockwood H, Reynaud J, Gardiner S, et al. Lamina cribrosa microarchitecture in normal monkey eyes part 1: methods and initial results. *Invest Ophthalmol Vis Sci*. 2015;56:1618–1637.
11. Yan DB, Coloma FM, Metheetrairut A, et al. Deformation of the lamina cribrosa by elevated intraocular pressure. *Br J Ophthalmol*. 1994;78(8):643–648.
12. Burgoyne CF. A biomechanical paradigm for axonal insult within the optic nerve head in aging and glaucoma. *Exp Eye Res*. 2011;93:120–132.
13. Campbell IC, Coudrillier B, Ross Ethier C. Biomechanics of the posterior eye: a critical role in health and disease. *J Biomech Eng*. 2014;136:021005.
14. Sigal IA, Flanagan JG, Ethier CR. Factors influencing optic nerve head biomechanics. *Invest Ophthalmol Vis Sci*. 2005;46:4189–4199.
15. Sigal IA, Ethier CR. Biomechanics of the optic nerve head. *Exp Eye Res*. 2009;88:799–807.
16. Burgoyne CF, Downs JC, Bellezza AJ, et al. The optic nerve head as a biomechanical structure: a new paradigm for understanding the role of IOP-related stress and strain in the pathophysiology of glaucomatous optic nerve head damage. *Prog Retin Eye Res*. 2005;24:39–73.
17. Crawford Downs J, Roberts MD, Sigal IA. Glaucomatous cupping of the lamina cribrosa: a review of the evidence for active progressive remodeling as a mechanism. *Exp Eye Res*. 2011;93:133–140.
18. Downs JC, Roberts MD, Burgoyne CF. Mechanical environment of the optic nerve head in glaucoma. *Optom Vis Sci*. 2008;85:425–435.
19. Furlanetto RL, Park SC, Damle UJ, et al. Posterior displacement of the lamina cribrosa in glaucoma: in vivo interindividual and intereye comparisons. *Invest Ophthalmol Vis Sci*. 2013;54:4836–4842.
20. Jung KI, Jung Y, Park KT, Park CK. Factors affecting plastic lamina cribrosa displacement in glaucoma patients. *Invest Ophthalmol Vis Sci*. 2014;55:7709–7715.
21. Ren R, Yang H, Gardiner SK, et al. Anterior lamina cribrosa surface depth, age, and visual field sensitivity in the Portland Progression Project. *Invest Ophthalmol Vis Sci*. 2014;55:1531–1539.
22. Levy NS, Crapps EE. Displacement of optic nerve head in response to short-term intraocular pressure elevation in human eyes. *Arch Ophthalmol*. 1984;102:782–786.
23. Yang H, Downs JC, Girkin C, et al. 3-D histomorphometry of the normal and early glaucomatous monkey optic nerve head: lamina cribrosa and peripapillary scleral position and thickness. *Invest Ophthalmol Vis Sci*. 2007;48:4597–4607.
24. Fatehee N, Yu PK, Morgan WH, et al. The impact of acutely elevated intraocular pressure on the porcine optic nerve head. *Invest Ophthalmol Vis Sci*. 2011;52:6192–6198.
25. Strouthidis NG, Fortune B, Yang H, et al. Longitudinal change detected by spectral domain optical coherence tomography in the optic nerve head and peripapillary retina in experimental glaucoma. *Invest Ophthalmol Vis Sci*. 2011;52:1206–1219.
26. Roberts MD, Liang Y, Sigal IA, et al. Correlation between local stress and strain and lamina cribrosa connective tissue volume fraction in normal monkey eyes. *Invest Ophthalmol Vis Sci*. 2010;51:295–307.
27. Roberts MD, Sigal IA, Liang Y, et al. Changes in the biomechanical response of the optic nerve head in early experimental glaucoma. *Invest Ophthalmol Vis Sci*. 2010;51:5675–5684.
28. Sigal IA. Interactions between geometry and mechanical properties on the optic nerve head. *Invest Ophthalmol Vis Sci*. 2009;50:2785–2795.
29. Sigal IA, Yang H, Roberts MD, et al. IOP-induced lamina cribrosa displacement and scleral canal expansion: an analysis of factor interactions using parameterized eye-specific models. *Invest Ophthalmol Vis Sci*. 2011;52:1896–1907.
30. Spaide RF, Koizumi H, Pozzoni MC. Enhanced depth imaging spectral-domain optical coherence tomography. *Am J Ophthalmol*. 2008;146:496–500.
31. Wang B, Nevins JE, Nadler Z, et al. In vivo lamina cribrosa micro-architecture in healthy and glaucomatous eyes as assessed by optical coherence tomography. *Invest Ophthalmol Vis Sci*. 2013;54:8270–8274.
32. Nadler Z, Wang B, Wollstein G, et al. Repeatability of in vivo 3D lamina cribrosa microarchitecture using adaptive optics spectral domain optical coherence tomography. *Biomed Opt Express*. 2014;5:1114–1123.
33. Lee EJ, Kim TW, Weinreb RN, et al. Visualization of the lamina cribrosa using enhanced depth imaging spectral-domain optical coherence tomography. *Am J Ophthalmol*. 2011;152:87–95.e81.
34. Choma M, Sarunic M, Yang C, Izatt J. Sensitivity advantage of swept source and Fourier domain optical coherence tomography. *Opt Express*. 2003;11:2183–2189.
35. Sigal IA, Wang B, Strouthidis NG, et al. Recent advances in OCT imaging of the lamina cribrosa. *Br J Ophthalmol*. 2014;98(Suppl 2):ii34–ii39.
36. Park HY, Jeon SH, Park CK. Enhanced depth imaging detects lamina cribrosa thickness differences in normal tension glaucoma and primary open-angle glaucoma. *Ophthalmology*. 2012;119:10–20.
37. Park HY, Park CK. Diagnostic capability of lamina cribrosa thickness by enhanced depth imaging and factors affecting thickness in patients with glaucoma. *Ophthalmology*. 2013;120:745–752.
38. Park SC, Hsu AT, Su D, et al. Factors associated with focal lamina cribrosa defects in glaucoma. *Invest Ophthalmol Vis Sci*. 2013;54:8401–8407.
39. You JY, Park SC, Su D, et al. Focal lamina cribrosa defects associated with glaucomatous rim thinning and acquired pits. *JAMA Ophthalmol*. 2013;131:314–320.
40. Faridi OS, Park SC, Kabadi R, et al. Effect of focal lamina cribrosa defect on glaucomatous visual field progression. *Ophthalmology*. 2014;121:1524–1530.
41. Kiumehr S, Park SC, Syril D, et al. In vivo evaluation of focal lamina cribrosa defects in glaucoma. *Arch Ophthalmol*. 2012;130:552–559.

42. Barrancos C, Rebolleda G, Oblanca N, et al. Changes in lamina cribrosa and prelaminar tissue after deep sclerectomy. *Eye (Lond)*. 2014;28:58–65.
43. Lee EJ, Kim TW. Lamina cribrosa reversal after trabeculectomy and the rate of progressive retinal nerve fiber layer thinning. *Ophthalmology*. 2015;122:2234–2242.
44. Lee EJ, Kim TW, Weinreb RN, Kim H. Reversal of lamina cribrosa displacement after intraocular pressure reduction in open-angle glaucoma. *Ophthalmology*. 2013;120:553–559.
45. Park HY, Shin HY, Jung KI, Park CK. Changes in the lamina and prelamina after intraocular pressure reduction in patients with primary open-angle glaucoma and acute primary angle-closure. *Invest Ophthalmol Vis Sci*. 2014;55:233–239.
46. Reis AS, O'Leary N, Stanfield MJ, et al. Laminar displacement and prelaminar tissue thickness change after glaucoma surgery imaged with optical coherence tomography. *Invest Ophthalmol Vis Sci*. 2012;53:5819–5826.
47. Chakraborty R, Read SA, Collins MJ. Diurnal variations in axial length, choroidal thickness, intraocular pressure, and ocular biometrics. *Invest Ophthalmol Vis Sci*. 2011;52:5121–5129.
48. Johnstone J, Fazio M, Rojananuangnit K, et al. Variation of the axial location of Bruch's membrane opening with age, choroidal thickness, and race. *Invest Ophthalmol Vis Sci*. 2014;55:2004–2009.
49. Lee SW, Yu SY, Seo KH, et al. Diurnal variation in choroidal thickness in relation to sex, axial length, and baseline choroidal thickness in healthy Korean subjects. *Retina*. 2014;34:385–393.
50. Tan KA, Gupta P, Agarwal A, et al. State of science: choroidal thickness and systemic health. *Surv Ophthalmol*. 2016;61:566–581.
51. Lee SH, Yu DA, Kim TW, et al. Reduction of the lamina cribrosa curvature after trabeculectomy in glaucoma. *Invest Ophthalmol Vis Sci*. 2016;57:5006–5014.
52. Thakku SG, Tham YC, Baskaran M, et al. A global shape index to characterize anterior lamina cribrosa morphology and its determinants in healthy Indian eyes. *Invest Ophthalmol Vis Sci*. 2015;56:3604–3614.
53. Girard MJ, Strouthidis NG, Ethier CR, Mari JM. Shadow removal and contrast enhancement in optical coherence tomography images of the human optic nerve head. *Invest Ophthalmol Vis Sci*. 2011;52:7738–7748.
54. Girard MJ, Tun TA, Husain R, et al. Lamina cribrosa visibility using optical coherence tomography: comparison of devices and effects of image enhancement techniques. *Invest Ophthalmol Vis Sci*. 2015;56:865–874.
55. Mari JM, Strouthidis NG, Park SC, Girard MJ. Enhancement of lamina cribrosa visibility in optical coherence tomography images using adaptive compensation. *Invest Ophthalmol Vis Sci*. 2013;54:2238–2247.
56. Tun TA, Thakku SG, Png O, et al. Shape changes of the anterior lamina cribrosa in normal, ocular hypertensive, and glaucomatous eyes following acute intraocular pressure elevation. *Invest Ophthalmol Vis Sci*. 2016;57:4869–4877.
57. Kim YW, Kim DW, Jeoung JW, et al. Peripheral lamina cribrosa depth in primary open-angle glaucoma: a swept-source optical coherence tomography study of lamina cribrosa. *Eye (Lond)*. 2015;29:1368–1374.
58. Park SC, Brumm J, Furlanetto RL, et al. Lamina cribrosa depth in different stages of glaucoma. *Invest Ophthalmol Vis Sci*. 2015;56:2059–2064.
59. Li L, Bian A, Cheng G, Zhou Q. Posterior displacement of the lamina cribrosa in normal-tension and high-tension glaucoma. *Acta Ophthalmol*. 2016;94:e492–e500.
60. Kadziauskiene A, Kuoliene K, Asoklis R, et al. Changes in choroidal thickness after intraocular pressure reduction following trabeculectomy. *Acta Ophthalmol*. 2016;94:586–591.
61. Yang H, Williams G, Downs JC, et al. Posterior (outward) migration of the lamina cribrosa and early cupping in monkey experimental glaucoma. *Invest Ophthalmol Vis Sci*. 2011;52:7109–7121.
62. Kim YW, Jeoung JW, Girard MJ, et al. Positional and curvature difference of lamina cribrosa according to the baseline intraocular pressure in primary open-angle glaucoma: a swept-source optical coherence tomography (SS-OCT) study. *PloS One*. 2016;11, e0162182.
63. Kim YW, Jeoung JW, Kim DW, et al. Clinical assessment of lamina cribrosa curvature in eyes with primary open-angle glaucoma. *PloS One*. 2016;11, e0150260.
64. Lee SH, Kim TW, Lee EJ, et al. Diagnostic power of lamina cribrosa depth and curvature in glaucoma. *Invest Ophthalmol Vis Sci*. 2017;58:755–762.
65. Abe RY, Gracitelli CP, Diniz-Filho A, et al. Lamina cribrosa in glaucoma: diagnosis and monitoring. *Curr Ophthalmol Rep*. 2015;3:74–84.
66. Lee EJ, Kim TW, Weinreb RN. Reversal of lamina cribrosa displacement and thickness after trabeculectomy in glaucoma. *Ophthalmology*. 2012;119:1359–1366.
67. Lee EJ, Kim TW, Weinreb RN. Variation of lamina cribrosa depth following trabeculectomy. *Invest Ophthalmol Vis Sci*. 2013;54:5392–5399.
68. Girard MJ, Beotra MR, Chin KS, et al. In vivo 3-dimensional strain mapping of the optic nerve head following intraocular pressure lowering by trabeculectomy. *Ophthalmology*. 2016;123:1190–1200.
69. Quigley H, Arora K, Idrees S, et al. Biomechanical responses of lamina cribrosa to intraocular pressure change assessed by optical coherence tomography in glaucoma eyes. *Invest Ophthalmol Vis Sci*. 2017;58:2566–2577.
70. Radius RL. Regional specificity in anatomy at the lamina cribrosa. *Arch Ophthalmol*. 1981;99:478–480.
71. Hernandez MR. The optic nerve head in glaucoma: role of astrocytes in tissue remodeling. *Prog Retin Eye Res*. 2000;19:297–321.
72. Sigal IA, Yang H, Roberts MD, et al. IOP-induced lamina cribrosa deformation and scleral canal expansion: independent or related? *Invest Ophthalmol Vis Sci*. 2011;52:9023–9032.
73. Liu B, McNally S, Kilpatrick JI, et al. Aging and ocular tissue stiffness in glaucoma. *Surv Ophthalmol*. 2018;63:56–74.
74. Coudrillier B, Tian J, Alexander S, et al. Biomechanics of the human posterior sclera: age- and glaucoma-related changes measured using inflation testing. *Invest Ophthalmol Vis Sci*. 2012;53:1714–1728.
75. Geraghty B, Jones SW, Rama P, et al. Age-related variations in the biomechanical properties of human sclera. *J Mech Behav Biomed Mater*. 2012;16:181–191.
76. Girard MJ, Suh JK, Bottlang M, et al. Scleral biomechanics in the aging monkey eye. *Invest Ophthalmol Vis Sci*. 2009;50:5226–5237.
77. Grytz R, Fazio MA, Libertiaux V, et al. Age- and race-related differences in human scleral material properties. *Invest Ophthalmol Vis Sci*. 2014;55:8163–8172.
78. Vurgese S, Panda-Jonas S, Jonas JB. Scleral thickness in human eyes. *PloS One*. 2012;7, e29692.

79. Albon J, Karwatowski WS, Avery N, et al. Changes in the collagenous matrix of the aging human lamina cribrosa. *Br J Ophthalmol*. 1995;79:368–375.
80. Albon J, Purslow PP, Karwatowski WS, Easty DL. Age related compliance of the lamina cribrosa in human eyes. *Br J Ophthalmol*. 2000;84:318–323.
81. Sihota R, Sony P, Gupta V, et al. Diagnostic capability of optical coherence tomography in evaluating the degree of glaucomatous retinal nerve fiber damage. *Invest Ophthalmol Vis Sci*. 2006;47:2006–2010.
82. Kim S, Sung KR, Lee JR, Lee KS. Evaluation of lamina cribrosa in pseudoexfoliation syndrome using spectral-domain optical coherence tomography enhanced depth imaging. *Ophthalmology*. 2013;120:1798–1803.
83. Braunsmann C, Hammer CM, Rheinlaender J, et al. Evaluation of lamina cribrosa and peripapillary sclera stiffness in pseudoexfoliation and normal eyes by atomic force microscopy. *Invest Ophthalmol Vis Sci*. 2012;53:2960–2967.

Footnotes and Financial Disclosures

Originally received: November 20, 2017.
Final revision: May 9, 2018.
Accepted: May 9, 2018.
Available online: ■■■. Manuscript no. 2017-2608.

[1] Clinic of Ears, Nose, Throat and Eye Diseases, Institute of Clinical Medicine, Faculty of Medicine, Vilnius University, Vilnius, Lithuania.

[2] Vilnius University Hospital Santaros Klinikos, Vilnius, Lithuania.

[3] Department of Mathematical Statistics, Vilnius Gediminas Technical University, Vilnius, Lithuania.

[4] Singapore Eye Research Institute, Singapore National Eye Centre, Singapore.

[5] Ophthalmology & Visual Sciences Academic Clinical Program, Duke-NUS Medical School, Singapore.

[6] Department of Ophthalmology, Yong Loo Lin School of Medicine, National University of Singapore, Singapore.

[7] GePaSud Laboratory, University of French Polynesia, Tahiti, French Polynesia.

[8] Ophthalmic Engineering & Innovation Laboratory, Department of Biomedical Engineering, National University of Singapore, Singapore.

[9] Lee Kong Chian School of Medicine, Nanyang Technological University, Singapore.

[10] Department of Clinical Pharmacology, Medical University of Vienna, Vienna, Austria.

[11] Center for Medical Physics and Biomedical Engineering, Medical University of Vienna, Vienna, Austria.

Financial Disclosure(s):
The author(s) have no proprietary or commercial interest in any materials discussed in this article.

HUMAN SUBJECTS: This study includes human subject/tissues. Study protocol was approved by the Regional Research Ethics Committee. All tenets of the Declaration of Helsinki were followed. Informed consent was obtained from all human subjects.

No animal subjects were used in this study.

Author Contributions:

Conception and design: Kadziauskienė, Ašoklis, Lesinskas, Schmetterer

Data collection: Kadziauskienė, Jašinskienė, Ašoklis

Analysis and interpretation: Kadziauskienė, Lesinskas, Rekašius, Chua, Cheng, Mari, Girard, Schmetterer

Obtained funding: Not applicable

Overall responsibility: Kadziauskienė, Jašinskienė, Ašoklis, Lesinskas, Rekašius, Chua, Cheng, Mari, Girard, Schmetterer

Abbreviations and Acronyms:
BM = Bruch's membrane; **BMO** = Bruch's membrane opening; **CCT** = central corneal thickness; **CI** = confidence interval; **D** = diopters; **dB** = decibels; **GSI** = global shape index; **ICC** = intraclass correlation coefficient; **IOP** = intraocular pressure; **LC** = lamina cribrosa; **LCD** = lamina cribrosa depth; **MD** = mean deviation; **N-T** = nasal-temporal; **ONH** = optic nerve head; **POAG** = primary open-angle glaucoma; **RNFL** = retinal nerve fiber layer; **S-I** = superior-inferior; **VIF** = variance inflation factor; **VF** = visual field.

Correspondence:
Aistė Kadziauskienė, MD, Clinic of Ears, Nose, Throat and Eye Diseases, Institute of Clinical Medicine, Faculty of Medicine, Vilnius University, Vilnius University Hospital Santaros Klinikos, Santariskiu g. 2, LT-08661 Vilnius, Lithuania. E-mail: aistedam@gmail.com.